Experimental Aerodynamic Investigations on Commercial Aircraft High Lift Characteristics by Large Engine Nacelles

Ulrich Jung* and Christian Breitsamter†

Institute of Aerodynamics, Technische Universität München, 85748 Garching, Germany

Abstract

High by-pass engines are identified to be a feasible measure for transport aircraft to reduce noise and specific fuel consumption. However, the wing flow is strongly influenced by interference effects due to engine nacelle and pylon which potentially increase with larger nacelles. A detailed wind tunnel half model of a transport aircraft in approach configuration is used to investigate these effects. The aerodynamic coefficients of lift, drag, and pitching moment are obtained for various angles of attack. To investigate the effect of nacelle type on wing flow topology, wool tuft pictures are taken. The wing wake flow field is investigated by means of hot-wire anemometry. All tests are conducted in the low-speed wind tunnel facility A and C at TU München with Reynolds numbers between 0.5×10^6 and 1.0×10^6 based on wing mean aerodynamic chord. A current nacelle as well as two larger nacelles used for engines with increased by-pass ratios are consecutively installed. Significant differences in the wing and wake flow field are identified for the different nacelles installed. the maximum angle of attack decreases with increasing the nacelle diameter while the maximum lift coefficient is less affected due to optimized nacelle strakes.

1 Introduction

Turbojet engine by-pass-ratio tends to increase for future Commercial Transport Aircraft (CTA). The reason for this is based on two important objectives: Engine noise is reduced for increasing by-pass ratio through a decreased fan flow velocity [1] and fuel efficiency is increased by an increase of propulsion efficiency [2]. However, increasing the by-pass-ratio leads to a larger engine nacelle diameter. For nacelles mounted under the wing this increase in diameter causes a higher potential of the nacelle to disturb the flow on the wing, known as adverse aerodynamic interference effect. This is based on a corresponding closer coupling of engine and wing as well as generally the effect of the nacelle size.

*Diplom-Ingenieur, Research Engineer.

†Doktor-Ingenieur, Chief Scientist.

For the CTA approach condition high maximum lift coefficients are necessary to keep the approach velocity at moderate values. Regulations give a safety margin for lowest approach velocity being 23% higher than the stall speed. This requirement motivates to analyze the on set and progression of stall and the aim to maintain the maximum lift coefficient at a value as high as possible. To simulate these incompressible CTA approach flow conditions low-speed wind tunnel tests are appropriate.

2 Experimental Setup

To analyze the flow topology of an approaching CTA and specifically the influence of increasing engine size on the aerodynamic interference, experiments are conducted in the large low-speed wind tunnels A (WTA) and C (WTC) of the Institute of Aerodynamics - TU München (AER). Specifications of these wind tunnels can be found in [3].

The used wind tunnel model is representative for a modern twin engine CTA. This detailed half model comprises the right half of the fuselage as well as the right wing including high-lift elements and the engine nacelle installed under the wing, Fig. 1. Slat, flap and aileron deflection angles are chosen to represent the approach high-lift configuration. Three types of through-flow nacelles were consecutively installed. They represent jet engines of different bypass ratio (BPR), incorporating a conventional turbojet simulator as baseline (BL) (BRP ≈ 6), a Very High By-Pass Ratio (VHBR) simulator (BRP ≈ 8), and an Ultra High By-Pass Ratio (UHBR) simulator (BPR ≈ 11). All nacelles are fitted with one respectively two individually adjusted engine nacelle strakes (ENS) installed at the outer surface of the nacelle either inboard or inboard and outboard to enhance the stall characteristics of each configuration.

3 Results

3.1 Force Measurements

Force measurements were conducted in WTA with an open test section. The six-component underfloor balance measures steady state forces and moments, from which lift C_A, drag C_W and pitching moment C_M coefficients are calculated. Freestream velocities set to $U_\infty = 25m/s$, $40m/s$, and $50m/s$. This leads to Mach numbers of $Ma \approx 0.07$ to $Ma \approx 0.15$, representing incompressible flow conditions. The corresponding Reynolds number for these experiments based on mean aerodynamic chord varies in the range of $Re \approx 5 \times 10^5$ to 1×10^6. The angle of attack is varied from $\alpha = -10°$ to $25°$.

The resulting lift polar for VHBR configuration at different Re is shown in Fig. 2 (left). It becomes clear from this Reynolds number sensitivity study that the linear region is not significantly affected by Re variations. Larger c_{Amax} values arise from increased Reynolds number. Also, a larger $\alpha_{c,Amax}$ arise from increased Re. And finally, c_{Amax} tends to converge within the tested Re-range. If one compares the lift polars for the different nacelle configurations, Fig. 2 (right), a tendency of decreasing $\alpha_{c,Amax}$ results from an increased nacelle diameter. But there is no significant effect on c_{Amax}. This is due to optimized ENS as well as an adjusted 'Slat Krueger' adjacent to the VHBR as well as UHBR nacelles.

Figure 1: CTA half-model in WTA.

3.2 Wool Tuft Flow Visualization

To visualize the surface flow, wool tufts are attached to wing, fowler flap, aileron, nacelles, and nacelle pylon of the model. The wool tuft investigation is conducted for moderate angles of attack, typical for approach, as well as stall and post-stall angles of attack in WTA. The freestream velocity is $U_\infty = 25m/s$, leading to $Re \approx 5 \times 10^5$. Exemplarily, Fig. 3 compares the wool tuft pictures of BL and VHBR configurations at angles of attack, which indicate the beginning of stall. The observed phenomena are marked in the pictures.

Clear differences in the flow topology are observed for the two configurations. To start with BL-configuration: Advanced flow separation is detected at the inboard and outboard part of the aileron and on the pylon of the nacelle. The begin of separation is identified on inboard wing and flap kink. The following areas are influenced by turbulent flow of the ENS: The nacelle upper side and the wake area of ENS on upper wing surface.

For the VHBR configuration only the inboard and outboard part of the aileron are affected by advanced separation. Starting separation is observed for the inboard wing and the flap kink. Areas, which are influenced by the turbulent flow of the ENS are the nacelle's upper side and the wake area of ENS on upper wing surface.

3.3 Flow Field Investigation by Hot Wire Anemometry

By means of hot wire anemometry, the mean velocities as well as the velocity fluctuations of the wing's near wake flow field are investigated. The axial position of the near wake measurement

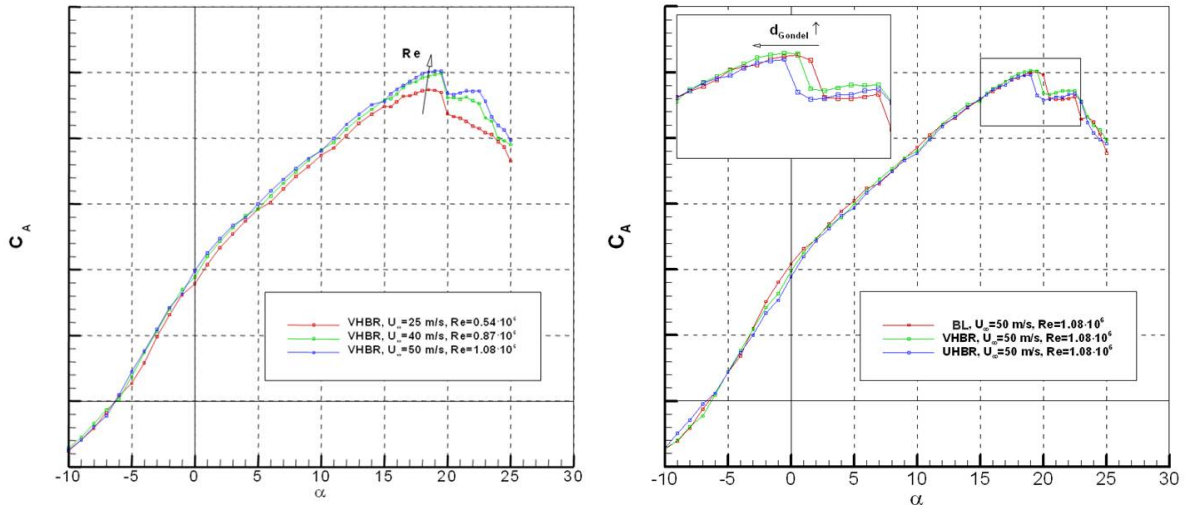

Figure 2: Lift polar for different Re and for different nacelles.

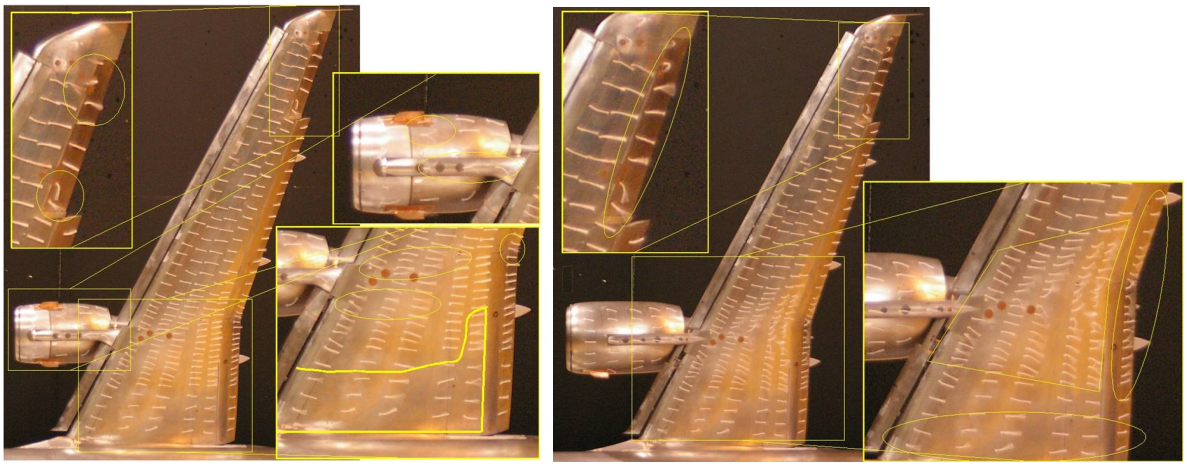

Figure 3: Wool tuft pictures for BL and VHBR configurations at beginning stall.

plane is $x* = x/b = 0.1$. In Fig. 4, the mean velocity fields are shown for BL, VHBR, and UHBR. The axial velocity deficit distribution $u/U_\infty < 1$ is color mapped. The direction and absolute values of the radial velocity components are represented by vectors.

The velocity deficit in the direct wake of the different nacelles is significantly affected by the configurations. The results from both larger nacelle configurations feature a significantly larger area of velocity deficit compared to the BL. Additionally, the shape of the zone of velocity deficit is different: For VHBR the nacelle wake is split into two deficit spots, whereas the deficit zone for UHBR is generally larger as well as linked up. The relevant areas are marked in the figure.

4 Conclusion

Low speed wind-tunnel tests with a detailed commercial transport aircraft model were conducted. In order to investigate interference effects between nacelle, pylon and wing, three different nacelles were considered for the investigations. Hereby, the effect of nacelle type configuration on longitudinal aerodynamic coefficients is investigated by force measurements. The

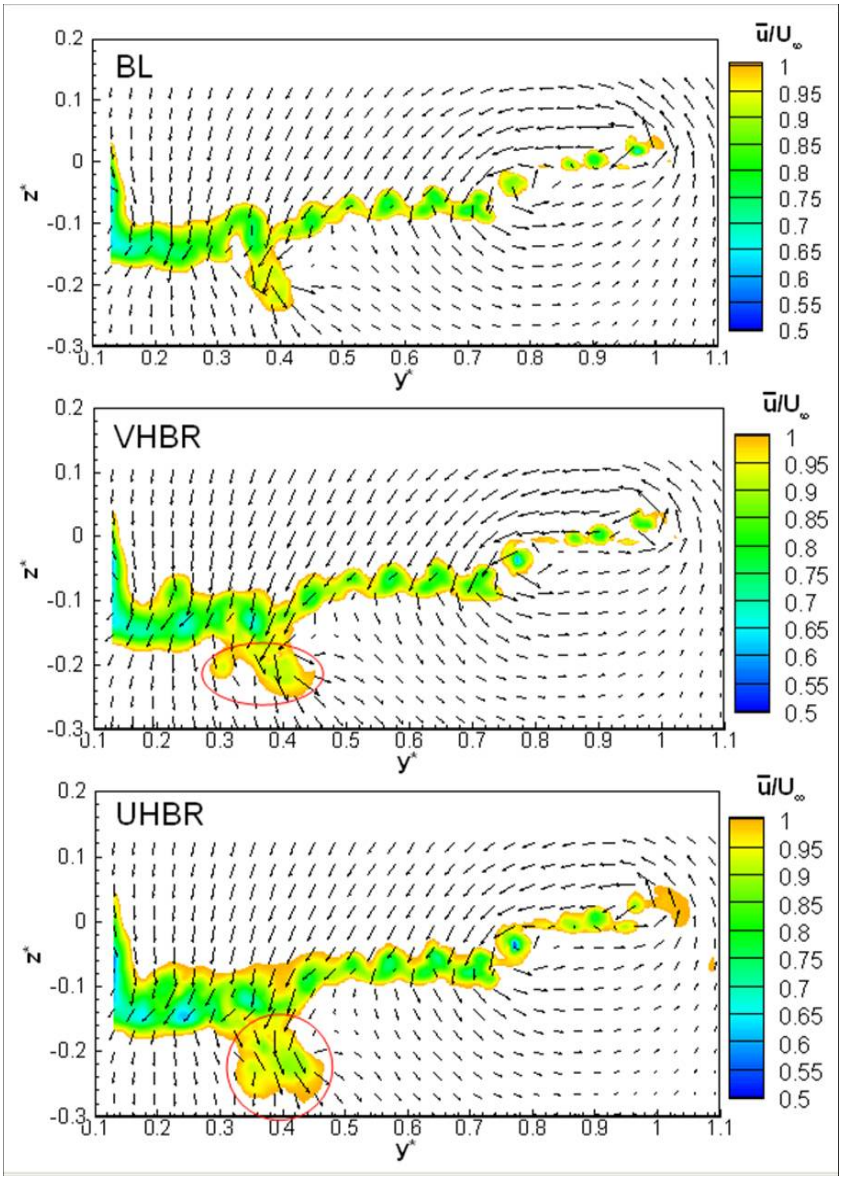

Figure 4: Wake velocity distribution for nacelle configurations BL, VHBR, and UHBR (from top to bottom).

flow topologies of the different configurations are studied by means of wool tuft pictures as well as hot-wire anemometry. Exemplarily, results of the investigations are presented. As a major outcome, it can be stated, that the investigated nacelle types have no significant effect on maximum lift coefficient due to optimized nacelle strake configurations, which is important for maintaining the minimum approach speed of the baseline configuration.

References

[1] Rüd, K.; Lichtfuss, H.J.: "Trends in Aero-Engine Development". In: Aspects of Engine-Airframe Integration for Transport Aircraft, Proceedings of the DLR Workshop Braunschweig, DLR-Mitteilung (Note) 96-01, 1996.

[2] Bräunling, W. J. G.: "Flugzeugtriebwerke". Second edition, S. 27, Springer Verlag, ISBN 3-540-40589-5, 2004.

[3] "Wind Tunnels". Institute of Aerodynamics - Technische Universität München, URL: http://www.aer.mw.tum.de/windkanal/index.en.php.